I.A.U. Karaj Branch

Journal of Applied Chemical Research, 9, 3, 73-84 (2015)

Journal of Applied Chemical Research

www.jacr.kiau.ac.ir

Mesoporous Carbon Modified with Iron Oxide Based Magnetic Nanomaterials for Removal of Malachite Green Dye From Aqueous Solution

Leila Torkian[1,*], Alireza J. Gholinezhad[2]

[1]Applied Chemistry Department, College of Basic Sciences, Islamic Azad University, South Tehran Branch, Tehran, Iran.

[2]Department of Applied Chemistry, Islamic Azad University, Central Tehran Branch, Tehran, Iran.

(Received 24 Dec. 2014; Final version received 27 Feb. 2015)

Abstract

Mesoporous carbon (CMK-3) modified with Fe3O4 nanoparticles has been successfully synthesized and characterized by powder X-ray diffraction (XRD), N2 adsorption-desorption, scanning electron microscope (SEM) and transmission electron microscopy (TEM).The results depict that the synthesized Fe-CMK-3 preserved the ordered mesoporous structure of CMK-3, and magnetic species were dispersed inside channels of CMK-3 as nanoparticles with the diameter of around 15 nm. When used as adsorbents, Fe-CMK-3 and CMK-3 exhibit excellent performance for removing Malachite Green dye from aqueous solutions. Effects of contact time, pH, initial dye and salt concentrations on dye removal efficiency were investigated. Due to the facility of the separation process with an external magnetic field, Fe-CMK-3 is suggested as a novel adsorbent for the removal of MG dye from aqueous solutions

Keywords: *Mesoporous carbon, Fe-CMK-3, Adsorption, Malachite Green.*

Introduction

Organic dyes are widely applied in textiles, paper, plastics, leather, food and cosmetic industry to color their products. They are an integral part of many industrial effluents and demand an appropriate method to dispose them off [1]. Most commercial dyes are chemically stable and are difficult to be removed from wastewater [2]. At present, more than 10,000 dyes have been effectively commercialized [3]. The release of colored waste water from these industries may present an eco-toxic hazard and introduce the potential danger of bioaccumulation, which may eventually affect

***Corresponding author:** Leila Torkian, Applied Chemistry Department, College of Basic Sciences, Islamic Azad University, South Tehran Branch, E-mail:ltorkian@azad.ac.ir.*

man through the food chain.

Various techniques like coagulation and precipitation, ion exchange, nano filtration, photo degradation, membrane separation, chemical oxidation and adsorption have been used for the removal of toxic pollutant from wastewater [4-9]. Among the numerous techniques, direct adsorption of the dye onto an appropriate medium could be superior and is known as an efficient and general dye removal method [10].Over the years, a number of workers have used different waste materials in the adsorption technique. They have studied the feasibility of using various materials, such as waste orange peel [11], banana pith [12], cotton waste, rice husk [13-14], bentonite clay[16], neem leaf powder [17], perlite [18], etc. as adsorbents for removal of various dyes from wastewaters, but they suffer from insufficient performance[15].

Recently, extensive studies have been focused on mesoporous carbon within the CMK-3 network as a good candidate for adsorption of some dyes [19-23]. In spite of the large specific surface area, large pore volumes, regular and tunable pore size, chemical inertness and good mechanical stability, the separation of carbon materials from the final solution is difficult, even causing secondary pollution [24]. Recent researchers have suggested that incorporation of magnetic components in to mesoporous carbon materials may enhance the separation and recovery of materials by conveniently applying external magnetic fields [25-27].

In the present work, the potential of magnetic mesoporous carbon composite Fe-CMK-3 for the removal of Malachite Green dye from aqueous solutions was investigated, for the first time. Malachite Green, (MG) is a water pollutant and conventionally used for materials such as silk, leather and paper. The toxicity of this triarylmethane dye, leads to the necessity of its treatment [28]. The effect of contact time, pH, initial concentration, and electrolyte on adsorption characteristics of Fe-CMK-3 was studied.

Experimental

Materials and methods

Triblock copolymer P123 ($EO_{20}PO_{70}EO_{20}$, EO = ethylene oxide, PO = propylene oxide, 5800) was supplied from Aldrich Co. Tetraethyl orthosilicate [TEOS, $Si(OC_2H_5)_4$], sucrose, NaCl, NaOH, HCl, $Fe(NO_3)_3.9H_2O$, glycol, ethanol and 4-[(4-dimethylaminophenyl) phenyl-methyl]-N,N-dimethylaniline (Malachite Green, $C_{23}H_{25}ClN_2$) were purchased from Merck (Germany).

Preparation of adsorbent

The mesoporous silica template SBA-15 was prepared according to the literature [29]. Mesoporous carbon material CMK-3 was prepared by using SBA-15 as hard template and sucrose as carbon source [30]. The magnetic mesoporous carbon Fe-CMK-3 was

prepared using ordered mesoporous carbon CMK-3 as the support, Fe $(NO_3)_3.9H_2O$ as the iron source and glycol as the reducing agent [31]. In a typical synthesis, 1 g CMK-3 was mixed homogenously with 5 g ethanol solution containing 0.7 mmol $Fe(NO_3)_3.9H_2O$, followed by drying in air at 100° C. Then dried sample was impregnated with 5 ml glycol. The mixture was calcined in N_2 at 250° C for 2 h to enable the formation of magnetic nanoparticles.

Characterization of adsorbent

The textural properties of adsorbent were determined by using the nitrogen sorption technique. The nitrogen adsorption–desorption isotherms were measured at -196 ◦C using a Micromeritics ASAP 2000 analyser. Prior to the measurement, sample degassed for 5 h at 70 ◦C. The specific surface area was calculated according to the BET (Brunauer–Emmet and Teller) model [32] while the pore size and pore volume were calculated using the Barrett–Joyner–Halenda (BJH) formula [33] based on the desorption branch of the isotherm. The mesoporous structure of the sample was investigated using X-ray powder diffraction (XRD).The X-ray Diffraction patterns were obtained at room temperature on a Bruker D8 diffractometer with a CuKα (0.15406 nm) radiation source in the 2θ range from 0.5 to 5, with a step size of 0.02◦. Transmission electron microscopy (TEM) was performed on Philips (CM 120) electron microscope. UV-visible absorption spectra were recorded using a UV-visible spectrophotometer (BIO-TEK KONTRON 923). The samples were placed in a quartz cuvette, and spectra were recorded at room temperature.

Adsorption equilibrium experiments

MG was selected as a model of weakly biodegradable pollutant to study the absorption behavior of Fe-CMK-3 and compare it with CMK-3. Effects of contact time, initial dye concentration, solution pH, temperature and electrolyte for the adsorption of MG dye on Fe-CMK-3 and CMK-3 adsorbents were investigated. In All experiments except for the initial concentration, 50 mg of absorbent was added to 25 ml water solution of the dye with a concentration of 1000mg/l. After stirring on a shaker for predetermined time intervals, the solution was treated with centrifugation for solid-liquid separation. The residual concentration of dye solution was determined using a calibration curve prepared at the corresponding maximum wavelength (500 nm) using a UV–visible spectrometer (Unicol Instrument Co., Ltd.). The amount of adsorbed dye, Q (mg/g), was calculated by:

$$q_e = \frac{(C_0 - C_e)V}{W} \qquad (1)$$

where C_0 and C_e are the initial and equilibrium concentrations (mg/L), respectively, V is the volume of dye solution (mL) and W is

the weight (g) of cmk-3 adsorbent. The dye removal efficiencies under different conditions were calculated from the difference between the initial (without adsorbent) and equilibrium concentrations of the solution.

The effect of pH on dye removal was studied over a pH range of 2 to 11. The initial pH of the dye solution was adjusted by the addition of 1 N solution of HCl or NaOH. The concentration of MG dye solution ranged from 50 -1000 mg/L to investigate the effects of dye concentration. The sorption studies were also carried out at different temperatures (30, 40, 50 and 60 °C) to determine the effect of temperature on the adsorption performance of adsorbents.

Results and discussion

Characterization of adsorbent

XRD

Figure 1 depicts small angle XRD patterns of the prepared CMK-3 and Fe-CMK-3. The CMK-3 displayed three distinct peaks with 2 theta at 0.82°, 1.46° and 1.7° indexed at (1 0 0), (1 1 0) and (2 0 0) reflections, suggesting the p6mm hexagonal symmetry of mesoporous structure. After the introduction of magnetic species, the reflection intensity of (1 0 0) diffraction peak got weakened and broadened and (1 1 0) and (2 0 0) peaks disappeared, which indicated that magnetic particles had interred into the channels of CMK-3 [34].

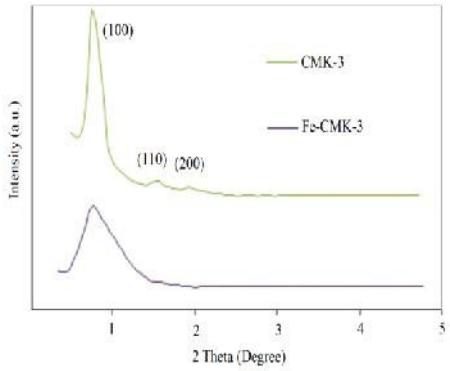

Figure 1. Low-angle X-ray diffraction patterns of prepared CMK-3 and Fe-CMK-3.

The wide angle XRD pattern of Fe-CMK-3 is shown in Figure 2. A relatively wide diffraction peak appeared at 2 theta of 25°, corresponding to the dispersing diffraction peak of amorphous carbon. Diffraction peaks at 2 theta of 30.1°, 35.4°, 43.1°, 57.0°, 62.6° and 75.3°, corresponding to (2 2 0), (3 1 1), (4 0 0), (5 1 1), (4 4 0) and (5 3 3) reflections, indicated that iron was present in the form of face-centered cubic phase Fe_3O_4 (JCPDS No. 85-1436) mainly on the support.

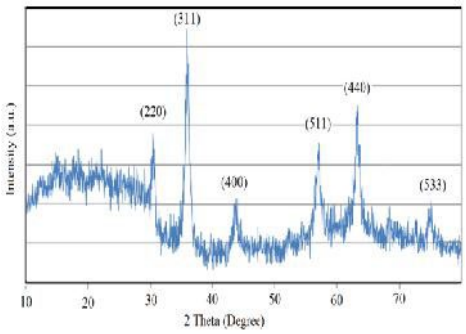

Figure 2. Wide angle X-ray diffraction pattern of prepared Fe-CMK-3.

N_2 adsorption/desorption

Figure 3 shows N_2 adsorption/desorption isotherms of prepared CMK-3 and Fe-CMK-3, as well as pore size distributions curves obtained from the adsorption branch. Both isotherms exhibit type IV isotherm of mesoporous materials according to classification of IUPAC with H1 hysteresis loops. The relatively steep nitrogen uptake step in isotherm located at P/P_0 between 0.4 and 0.9 indicating that samples have typical mesostructure with uniform size. The pore-size distribution curve calculated from the adsorption branch clearly confirms a narrow pore-size distribution. The average pore diameter of CMK-3 is 3.28 nm. After magnetic Fe oxide species were incorporated into the support, the pore size distribution broadened appreciably, but the average pore diameter is still 3.28 nm. The introduction of the Fe oxide species led to a distinct decrease in BET surface area (from 390.29 to219.6 m^2g^{-1}) and pore volume (from 0.6821 to 0.3542 cm^3g^{-1}). Three reasons have been suggested for the decrease: (i) Introduction of the magnetic Fe_3O_4 species into channels resulted in partially space occupation of pores and even blocking the micropores; (ii) Generation of oxidative gases from the thermal decomposition of Fe $(NO_3)_3$ ruined the carbon skeleton; (iii) Decomposition of Fe $(NO_3)_3$ and reduction of Fe species caused the loss of carbon atoms [35].

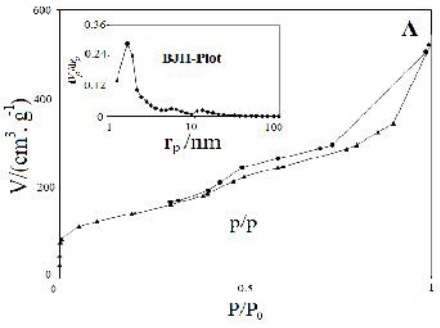

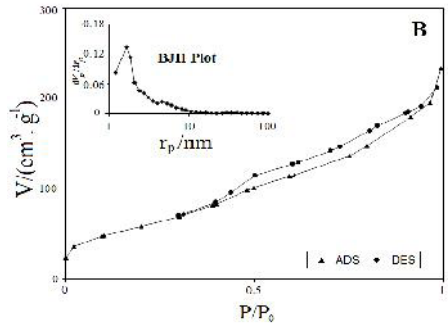

Figure 3. N_2 adsorption-desorption isotherms and porosity distribution (inset) of CMK-3 (A) and Fe-CMK-3

SEM

In Figure 4, SEM images of CMK-3 and Fe-CMK-3 are compared. Both had similar wheatlike morphology, indicating that the loading of Fe_3O_4 species did not affect the morphology of CMK-3. No significant aggregation of Fe oxide species was observed on the surface of the support in Figure 4B, suggesting that magnetic nanoparticles have been encapsulated inside the mesopores of CMK-3, which was in agreement with the XRD analysis and also previous reports [36].

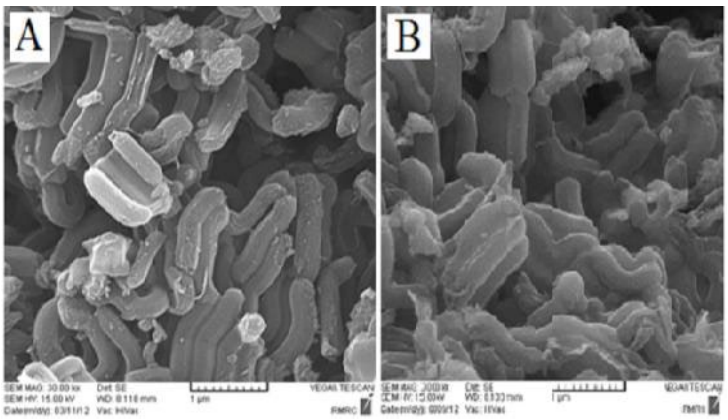

Figure 4. SEM images of CMK-3 (A) and Fe-CMK-3 (B).

TEM

Transmission electron microscopy of the CMK-3 (Figure 5A) shows the mesoporous structure with stripe like patterns in large domains. The visible dark spots with less than 15 nm size in TEM image of Fe-CMK-3 (Figure 5B) are Fe_3O_4 nanoparticles incorporated into the carbon framework. Large domain of highly ordered structure in Figure 5B depicts that after loading the Fe_3O_4 nanoparticles, the 2-D hexagonal mesostructure is well preserved in agreement with the low angle XRD characterization and SEM results.

Study of important parameters on the adsorption of MG dye by CMK-3 and Fe-CMK-3 adsorbents

Effect of contact time

The effect of contact time for the adsorption of MG dye on CMK-3 and Fe-CMK-3 was investigated for a period of 2 h for initial dye concentration of 1000mg/l.

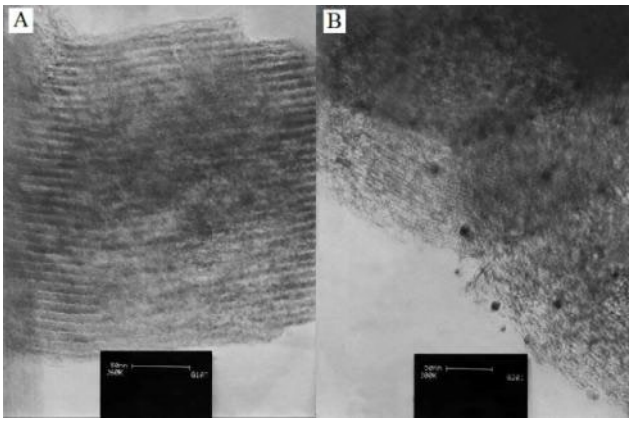

Figure 5. TEM images of CMK-3 (A) and Fe-CMK-3 (B).

As seen in Figure 6, it is evident that time has significant influence on the adsorption of dye. It can be seen that the adsorption of MG dye was quite rapid in the first 30 min, then gradually increased with the prolongation of contact time. Also CMK-3 shows more adsorption capacity than Fe-CMK-3. After 60 min of contact, no obvious variation in dye adsorbed was obvious and both adsorbents depicted similar capacities. Based on these results, 60 min was taken as the equilibrium time in batch adsorption experiments.

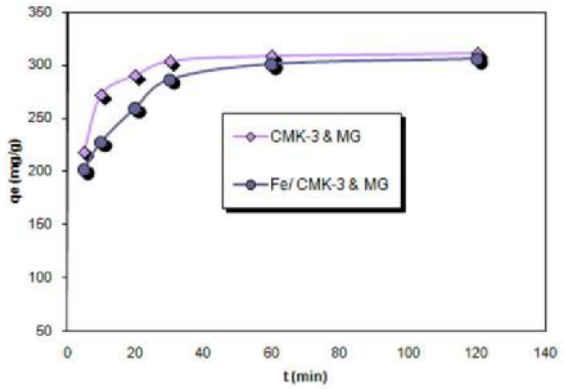

Figure 6. Effect of contact time on removal of MG dye by CMK-3 and Fe-CMK-3 (initial dye concentration: 1000mg/l, adsorbent dosage: 50mg/25ml).

Effect of pH

To study the influence of solution pH on the adsorption capacities of Fe-CMK-3 and CMK-3 for MG dye at equilibrium conditions, experiments were carried out using various initial pHs varying from 2 to 11. As shown in Figure 7, increasing pH from 2.9 to 10.8 resulted in increasing the adsorption from 307.78 to 378.39 mg/g and 300.58 to 376.91 mg/g in the presence of Fe-CMK-3 and CMK-3, respectively. It seems that MG as a cationic dye adsorbs more effectively on the surfaces

of Fe-CMK-3 and CMK-3 in basic solutions due to the negatively charged surface of both adsorbents in higher pH values. Similar behavior of some cationic dyes has been reported elsewhere [36].

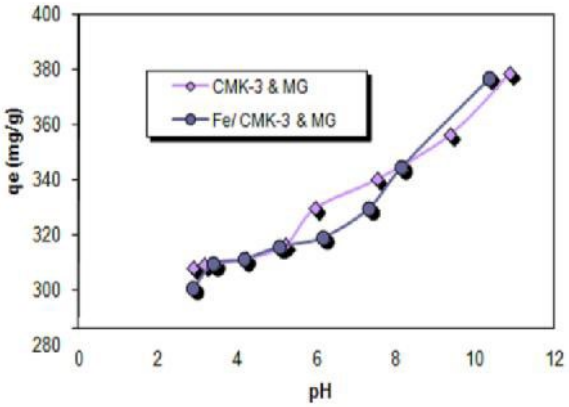

Figure 7. Effect of pH on removal of MG dye by CMK-3 and Fe-CMK-3 (initial dye concentration: 1000mgl-1, adsorbent dosage: 50mg/25ml).

Effect of initial dye concentration

The adsorption experiments were carried out in initial dye concentration range of 50-1000 mg/l. Figure 8 shows the effect of the initial concentration of MG on the amount adsorption in the presence of CMK-3 and Fe-CMK-3. When the dye concentration was increased from 50 to 1000 mg/l, the sorption capacity of CMK-3 and Fe-CMK-3 at equilibrium increased from 20.91 and 20.21 to 307.78 and 300.58 mg/g, respectively. This is attributable to the increase in the driving force of the concentration gradient with the higher initial dye concentration.

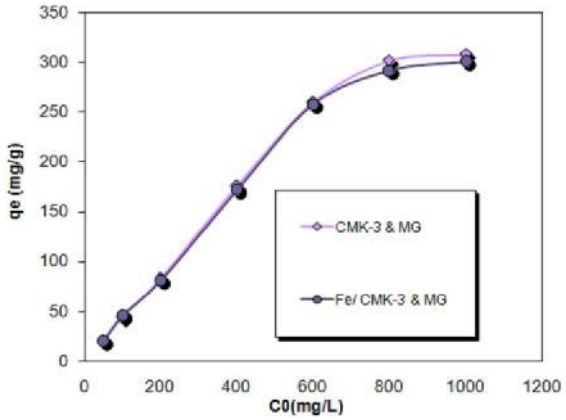

Figure 8. Effect of initial dye concentration on removal of MG dye by CMK-3 and Fe-CMK-3.

The amount of MG adsorbed on both adsorbents gradually increases with the dye concentration. The dye adsorption on Fe-CMK-3 and CMK-3 quickly reaches 84% (257.6 mg/g) of the total capacity at lower concentrations below 600 mg/L, while further increase in dye concentration from 600 to 1000 mg/L resulted in an increased adsorbed amount of 16%. Thus both CMK-3 and Fe-CMK-3 adsorbents exhibit very high adsorption capacities at below 600 mg/L concentrations of MG dye. Dye removal efficiency was higher for low initial concentrations because of the availability of unoccupied binding sites on the adsorbents. Percent color removal decreased with increasing dye concentration because of nearly complete coverage of the binding sites at high dye concentrations.

The maximum dye adsorption capacities for CMK-3 and Fe-CMK-3 were nearly 307 and 300 mg/g, respectively. The adsorption capacity of a given porous carbon strongly depends on the pore texture. The incorporation of iron oxide nanoparticles into CMK-3 mesostructure restricts the utility of a few pores, resulted in slightly lower adsorption capacity of Fe-CMK-3 compared to CMK-3.

Effect of electrolyte (sodium chloride) concentration

Wastewaters that contain dyes commonly include significant quantities of salts, thus the effect of electrolyte on MG removal needs to be investigated. Figure 9 illustrates the effect of NaCl on the amount of MG at an initial MG concentration of 1000 mg /l at 30 °C and solution pH. It can be seen that adsorption of MG on CMK-3 and Fe-CMK-3 adsorbents increased with increasing NaCl concentration. The presence of electrolyte may have two opposite effects. First, they may cause the neutralization of surface charge of adsorbent while competing with dye for surface adsorption.

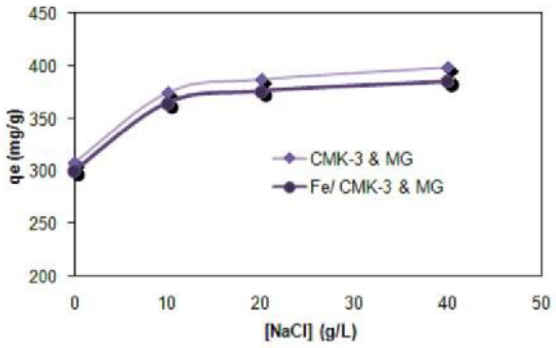

Figure 9. Effect of electrolyte on removal of MG dye by CMK-3 and Fe-CMK-3 (initial dye concentration: 1000mgl-1, adsorbent dosage: 50mg/25ml)**.**

With the increasing ionic strength, the adsorption capacity decreases due to screening of the surface charges. Secondly, the salt may decrease the degree of dissociation of the dye molecules and facilitate transport of dye to the adsorbent phase. The later effect seems to be dominant in this case and causes higher degree of dye adsorption on both mesoporous adsorbents [35].

Effect of temperature on the adsorption

The maximum adsorption capacity of MG adsorption on the prepared CMK-3 and Fe-CMK-3 versus the temperature is shown in Figure 10. It was found that the adsorption capacity of CMK-3 and Fe-CMK-3 decreased from 307.8 and 300.6 to 284.67 mg g^{-1} and 275.08 mg g^{-1}, respectively, with increasing in temperature from 30°C to 60°C, indicating the exothermic nature of the adsorption reactions. It can be explained that as temperature increased, the physical bonding between the organic compounds (including dyes) and the active sites of the adsorbent weakened. Besides, the solubility of MG also increased which caused the interaction forces between the solute and the solvent to become stronger than solute and adsorbent, therefore the solute was more difficult to adsorb. Similar behavior also reported elsewhere [33].

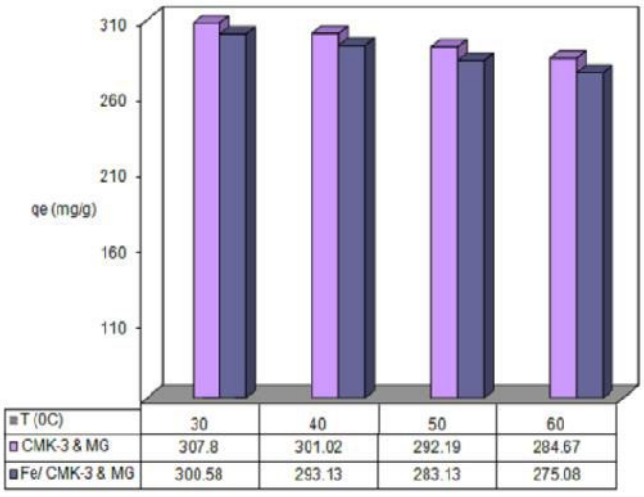

Figure 10. Effect of temperature on removal of MG dye by CMK-3 and Fe-CMK-3 (initial dye concentration: 1000mgl-1, adsorbent dosage: 50mg/25ml).

Conclusions

In this work we demonstrate the successful synthesis of a novel mesoporous carbon functionalized with magnetic nanoparticles, and its efficient absorbability. N_2 absorption and XRD results depicts that the synthesized Fe-CMK-3 possesses highly ordered mesostructure with 2-D hexagonal symmetry and its specific surface area and average pore diameter found to be 219.61m^2/g and

3.28nm respectively. Batch adsorption of MG dye on the mesoporous carbon indicate that the adsorption process is fast enough, as maximum removal take place within 60 min of contact time and removal efficiency of dye is improved in basic solutions. The adsorption of dye increased with increasing initial dye and salt concentrations. Although CMK-3 shows slightly higher adsorption capacity than Fe-CMK-3, but because of the facility of the separation process with an external magnetic field the latter is suggested for the removal of MG from aqueous solutions.

Acknowledgements

The authors thank the Office of the Vice-President for Research Affairs at South and North Tehran Branches, Islamic Azad University and the Research Center of Modeling and Optimization in Science and Engineering.

References

[1] S. Atef, *J. Environ. Science*, 5 (3), 197 (2009).

[2] M. Nassar, and Y. Magdy, *Chem. Eng. J.,* 66, 223 (1997).

[3] R. Gong, M. Li, C. Yang, *J. Hazard. Mater.,* 121, 247 (2005).

[4] R. Stephenson and J. Sheldon, *Water Res*., 30, 781 (1996).

[5] M. Chiou, and G. Chuang, *Chemosphere*, 62, 731 (2006).

[6] I. Salem, and M. El-maazawi, *Chemosphere*, 41, 1173 (2000).

[7] X. Wei, X. Kong., C. Sun *J., Chem. Eng. J.*, 223, 172-182 (2013).

[8] L. Torkian and E. Amereh, *Res. J. Chem. Environ.,* 15, 275-279 (2011).

[9] H. Jirankova, J. Mrazek, P. Dolecek *Desal. Wat. Treat*., 20, 96-101 (2010).

[10] G. Liu., S. Zheng, D. Yin, Z. Xu, , *J. Colloid Interface Sci*., 302, 47-53 (2006).

[11] C. Namasivayam, N. Muniasamy,; K. Gayatri,; M. Rani, *Bioresour. Technol*., 57, 37 (1996).

[12] C. Namasivayam, D. Prabha, and M. Kumutha, *Bioresour. Technol*., 64, 77 (1998).

[13]A. Daifullah, B. Girgis, and H. Gad, *Materials Letters*, 57, 1723 (2003).

[14] A. DaifullahGad, and B. Girgis, *J. Anal. Chem*., 13, 73 (2004).

[15] A. Daifullah, B. Girgis, and H. Gad, *Colloids and Surfaces A: Physicochem. Eng. Aspects*, 235, 1 (2004).

[16] K. Ramkrishna, and T. Viaraghavan, *Water Sci. Technol*., 36,189 (1997).

[17] K. Bhattacharya, and A. Sharma, *Dyes Pigm.,* 65, 51 (2005).

[18] M. Dogan, M. Alkan, A. Turkyilmaz, Y. Ozdemir, *J. Hazard. Mater*., 109, 141 (2004).

[19] M. Anbia, A. Davijani, *A. Chem. Eng. J.,* 223, 899 (2013).

[20] K. Vipin, M. Andrade, M.L. Pinto, *Purific. Technol*., 75, 366 (2010).

[21] N. Mohammadi,H. Khani, V. Gupta, *J.*

Colloid Interface Sci., 362, 457 (2011).

[22] J. Galan, A. Rodriguez, *Chem. Eng. J.*, 219, 62 (2013).

[23] S.E. Moradi, *J. Indust. Eng. Chem., In Press*.

[24] Y. Chi, W. Geng, L. Zhao, *J Colloid Interface Sci*., 369, 366 (2012).

[25] J. Chun, H. Lee, *Chemosphere*, 89, 1230 (2012).

[26] M. Dai, B.D. Vogt, *J. Colloid Interface Sci*., 387, 127 (2012).

[27] N. Farzin Nejad, E. Shams, Amini M.K.; *Fuel. Process. Technol*., 106,3756 (2013).

[28] D. Zhao, J. Feng, Q. Huo, N. Melosh, G.H. Fredrickson, B.F. Chmelka, *Science*, 279, 548 (1998).

[29] S. Jun, S.H. Joo, *J. Am. Chem. Soc*. 122, 10712 (2000).

[30]L. Hu, S. Dang, X. Yang *Microporous Mesoporous Mater*., 147, 188 (2012).

[31] S. Brauner, P.H., Emmet, E. Teller,. *J. Am. Chem. Soc*., 60, 309 (1983).

[32] E.P. Barrett, L.G. Joyner, *J. Am. Chem. Soc*., 73, 373 (1951).

[33]Y. Dong, H. Lin, F. Qu*, Chem. Eng. J.*, 194, 169 (2012).

[34]P.N. Palanisamy, P. Sivakumar, *Desalination*, 249, 388 (2009) .

[35]Z. Wang, X. Liu, M. Lv. *Mater. Lett*. 64, 1219 (2010).

[36] M. Alkan, M. Doğan, M.; Y. Turhan, *Chem. Eng. J.* ,139, 213 (2008).

.